Desalination and Water Treatment
www.deswater.com
doi: 10.5004/dwt.2023.29757

303 (2023) 11–23
August

Box–Behnken multi-response modeling and optimizing of brackish water reverse osmosis brine treatment using electrodialysis reversal with tortuous flow path

Amir Afarinandeh[a], Hamed Rashidi[b,*], Leila Karimi[c], Kambiz Heidari[d], Amirreza Arashi[e]

[a]*Chemical Engineering Department, Payame Noor University, Tehran 1659639884, Iran, email: amir.afarinandeh@yahoo.com*
[b]*Chemical Engineering Department, Kermanshah University of Technology, Kermanshah, Iran, email: h_rashidi@kut.ac.ir*
[c]*Department of Chemical and Environmental Engineering, University of Arizona, Tucson, USA, email: lkarimi@arizona.edu*
[d]*Chemical Engineering Department, Payame Noor University, Tehran 1659639884, Iran, email: kambiz_1991@yahoo.com*
[e]*Engineering Department, Karpern Co., Tehran, Iran, email: amirreza.arashi@gmail.com*

Received 21 May 2023; Accepted 9 July 2023

ABSTRACT

One of the most important challenges of drinking water production using reverse osmosis (RO) is the management of the concentrated brine because of its large volume. Electrodialysis reversal (EDR) technology has the potential to be integrated with RO process to treat the RO brine stream and increase the water recovery of the hybrid treatment process. In this study, we treated brine wastewater from brackish water RO plant using an EDR stack with tortuous flow path. We designed the experiments utilizing the Box–Behnken method which was applied for modeling and optimization. We modeled the EDR energy consumption, desalination efficiency, ion flux as a function of voltage, feed flow rate, and initial feed electrical conductivity as main factors. The obtained correlations between the input and output variables were evaluated by different statistics tools. We also maximized the ion flux and desalination efficiency while minimizing the energy consumption using multi-response optimization methodology. The optimum values for applied voltage, flow rate, and initial conductivity were founded to be 7.7 V, 25 mL/min, and 13,000 μS/cm, respectively. At the optimal conditions, the desalination efficiency, ion flux and energy consumption were 8.69%, 15.25 mg/m²·s, and 0.81 Wh/L, respectively, which were very close to the predicted values.

Keywords: Electrodialysis reversal; Brackish water reverse osmosis; Box–Behnken; Energy consumption

1. Introduction

With the rapid growth of industries, the world has encountered a serious challenge of sustaining water supply with desired quantity and quality. Today, desalination of seawater and brackish water using reverse osmosis (RO) to produce freshwater is being applied in some countries as a matured and efficient process. Depending on the level of salinity of the source brackish water, the treatment process efficiency can vary from 60% to 85% [1]. Therefore, RO produces a significant volume of high salinity concentrated brines with total dissolved solids (TDS) ranging from 500 up to 50,000 ppm [2]. The disposal of the concentrated brine back into the environment without further treatment results in serious environmental disasters. Thus, it is highly important to use appropriate brine management strategies, such as process hybridization [3]. Electrodialysis reversal (EDR) is a promising technology for RO brine treatment due to its robustness for scaling and fouling [4].

Electrodialysis (ED) is a membrane-based system consisting of channels made up of alternating stacked anion

* Corresponding author.

exchange membranes (AEM) and cation exchange membranes (CEM). There are two ED-based scenarios for RO brine management: (I) diluting by means of a low salinity solution in a reverse ED stack [5,6], and (II) concentrating RO brine by applying electric potential difference in an ED stack [7–9]. In the first scenario, the stack is fed by two solutions with different salinity levels. The salinity gradient between the two solutions leads to the migration of ions from the concentrated solution to the diluted solution until equilibrium is reached. During this process, the chemical potential is directly converted into electrical potential which is called salinity gradient power (SGP) [10]. In the second scenario which is in line with the waste minimization goal, the ED stack is fed by RO brine flowing through both dilute and concentrate channels. Under electrical potential difference, anions and cations are driven through AEM and CEM, respectively, creating alternately separated diluted and concentrated flows [1]. Although treatment of highly concentrated RO brine stream has high potential of scaling of less soluble salts in the membrane process, EDR is still efficient because of periodic polarity reversal. Upon the electrodialysis reversal (EDR), the fouling and scaling agent are repelled back from the membrane surface, leading to self-cleaning and stability of the process [11,12]. Some studies revealed that salinity of wastewaters streams can be increased by up to 360% when processed by EDR [13].

Although, EDR has been used for wastewater treatment in industrial scale, such as South Bay Water Reclamation Plant (SBWRP) in the city of San Diego, CA [14,15], it still needs to be investigated more because of its lower energy efficiency for treatment of streams with high salinity.

To increase the application of EDR technology in industrial scale the desalination efficiency should be maximized while simultaneously the energy consumption should be minimized. In general, EDR performance greatly depends on various parameters such as applied voltage, temperature, feed velocity, feed concentration and composition [8,18–20], membrane type [16], and ED stack configuration [17]. Karimi and Ghassemi [21] studied the performance of ED by varying the applied voltage, feed velocity, and processing time in a 15-cell pairs stack in a batch process. They used response surface methodology (RSM), based on Box–Behnken design (BBD) aiming at optimizing desalination rate and energy consumption as the output variables. In another study, Wang et al. [22] investigated the reclamation of saline water with bipolar membrane electrodialysis. The central composite design was carried out for modeling of current efficiency and energy consumption as a function of applied voltage, initial concentration of saline water, and initial concentration of acid/base. Because EDR has a high potential for application in reducing the volume of RO brine as one of the effective concentrate management strategies. It is highly important to study the desalination efficiency and energy consumption of the EDR for designing hybrid RO-ED plants for industrial-scale applications.

This work concentrates on the multi-response modeling and improvement of the EDR process for the minimization of brackish water RO brine volume by means of BBD.

2. Material and methods

2.1. Experimental set-up description

The ED stack was constructed by two commercial CEM and AEM (Fujifilm Type 10) with the surface area of 200 cm^2. Two tortuous-shaped titanium electrodes with an effective area of 100 cm^2 were used. Two rubber tortuous-shaped gaskets and one Plexiglas spacer were placed between membranes to create and seal concentrate channels. Properties of the membranes and EDR stack used in this study are shown in Tables 1 and 2, respectively. The schematic of the experimental set-up and the position of the valves to control the flow direction before and after polarity reversal are shown in Fig. 1 and Table 3, respectively.

2.2. Experimental procedure

RO brines with three different TDSs were prepared and fed into an ED stack with tortuous path flow at different flow rates and under different electrical potentials. The desalination efficiency, ion mass flux and energy consumption were the output responses. Apart from the promotion of turbulency, the tortuous path leads to increasing contact time of the water and membrane surfaces. Prior conducting the experiments, the limiting current density (LCD) was determined to avoid water dissociation in the vicinity of the ion exchange membranes. Then the brine

Table 1
Specifications of Type 10 membranes obtained from Fujifilm Corporation

Fujifilm membranes	AEM (anion permselective)	CEM (cation permselective)
Reinforcement	Polyolefin	Polyolefin
Thickness dry (μm)	125	135
Resistance (Ω/cm^2)	1.7	2.0
Perm selectivity	95	99
Water permeation (mL/bar/m^2·h)	6.5	6.5
pH stability	1–13	1–13
Temperature stability (°C)	60	60
Area (cm^2)	100	100

Table 2
Specification of electrodialysis reversal stack

Body	Material body	Plexiglas
	Dimensions of the body (cm)	2 × 15 × 17
Electrode	Material of electrodes	Titanium
	Effective area (1 cm^2)	
	Number of electrodes	2
	Dimensions of spacer	6
Spacer	Type of spacer	Tortuous
	Thickness of spacer (mm)	2.27
	Material of gasket	Rubber
Gasket	Type of gasket	Tortuous
	Thickness (mm)	0.5

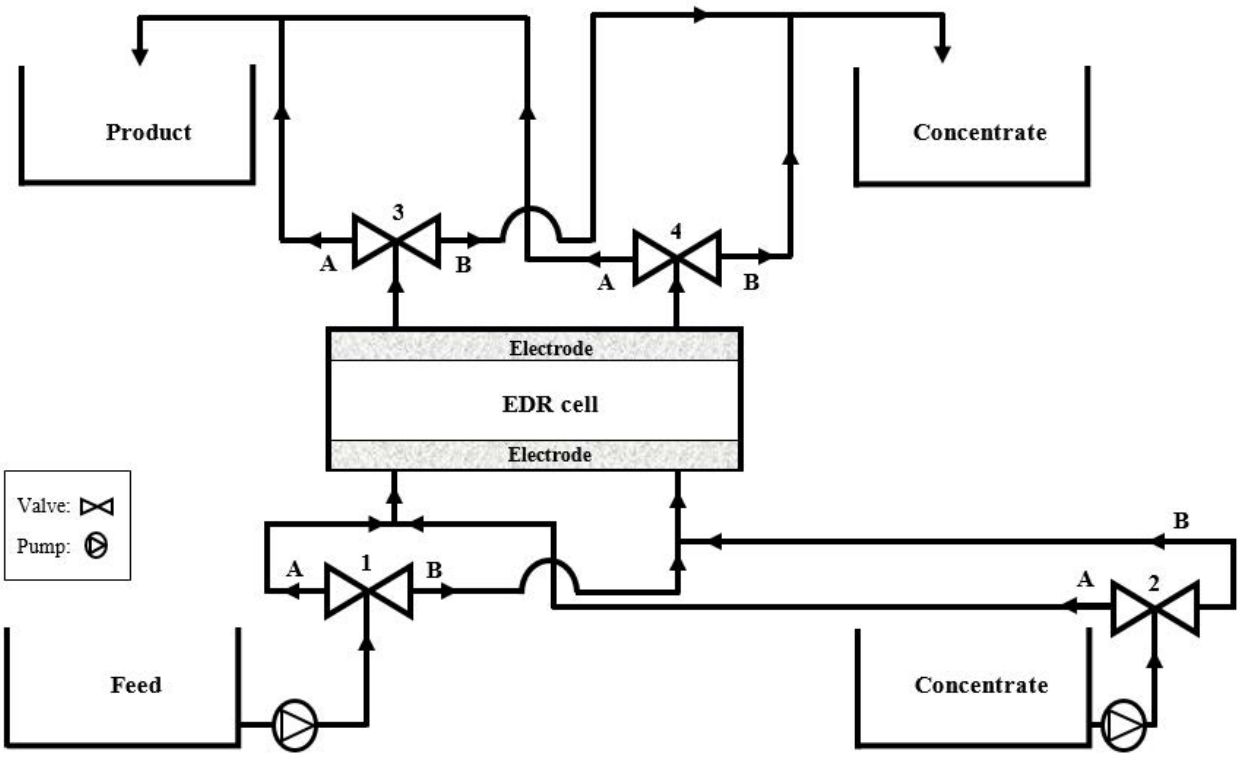

Fig. 1. Scheme of the electrodialysis reversal process for reverse osmosis brine minimization.

Table 3
Performance of valves and pumps in the electrodialysis reversal process

Valve number	Pathway of streams	
	Normal operation	Reversed operation
Valve 1	A	B
Valve 2	B	A
Valve 3	A	B
Valve 4	B	A

solutions with different electrical conductivities were made by diluting the RO brine with deionized water, which afterward were pumped into the EDR stack with tortuous path flow at different flow rates and under different electrical potentials. After 45 min electrodialytic brine treatment, the electric field direction was reversed for 15 min to clean up the surface of ion exchange membranes. The desalination efficiency, ion mass flux, and energy consumption were the output responses. All experiments were carried out at room temperature.

Electrical conductivity (EC) is a water quality criterion and a way of measuring the salinity level. The dilute stream EC was measured using a portable conductivity meter (Hanna HI8733 , Romania). Then the correlation between EC (μS/cm) and TDS (ppm) in room temperature is represented using Eq. (1) [23].

$$\mathrm{TDS} = k\mathrm{EC} \tag{1}$$

$$\mathrm{TDS} = 0.62\mathrm{EC} \tag{2}$$

where k increases with increasing ions variety in water and generally varies from 0.55 to 0.7 [20]. Herein, to adequately measure the value of TDS from EC, a linear regression equation [Eq. (2)] was obtained with R^2 of 0.9895. The desalination efficiency (R_1 (%)) was also measured using Eq. (3), where EC_i and EC_f are the initial and final electrical conductivity of the brine sample, respectively.

$$R_1 = \frac{\mathrm{EC}_i - \mathrm{EC}_f}{\mathrm{EC}_i} \times 100 \tag{3}$$

The ion mass flux (R_2 (mg/m^2·s)) was calculated using Eq. (4) as follows.

$$R_2 = \frac{\left(\mathrm{TDS}_i - \mathrm{TDS}_f\right) \times Q}{2S} \tag{4}$$

where TDS_i and TDS_f, Q, and S are the initial and final values of TDS (ppm), volume flow rate (mL/min), and the effective surface area of the ion exchange membranes, respectively.

The energy consumption (R_3 (Wh/L)) was also calculated by Eq. (5) as follows.

$$R_3 = \frac{V\bar{I}}{Q} \tag{5}$$

where Q is volume flow rate (L/h), V is the applied voltage and $\bar{I}$ is the average current (A), where is calculated by $\bar{I} = \frac{\int_0^t Idt}{t}$.

2.3. Characterization of RO brine

In this study, we used the brine wastewater obtained from brackish water RO plant (Kimia Daran Kavir, Yazd, Iran). The brine quality specifications at 25°C are summarized in Table 4.

2.4. Design of experiments

Three-factor BBD was applied to study and evaluate the effects of applied voltage, feed flow rate, and initial electrical conductivity of feed stream as the main input independent variables affecting three responses including desalination efficiency (%) (R_1), ion mass flux (mg/m²·s) (R_2), and energy consumption (Wh/L) (R_3) in the RO brine treatment using EDR. The input variables and their levels and design of experiments are presented in Tables 5 and 6, respectively. Thirteen experiments were designed with 5 times replication of the central point for each response. In this study, Design–Expert 0.0.11 software was employed to design the experiments as described in Table 6. To simultaneously maximize desalination efficiency and ion mass flux while minimizing energy consumption, all the input variable were justified to be in range.

3. Results and discussion

3.1. Results of limiting current density

Current density is an important operating parameter affecting the energy consumption and water recovery rate in the EDR process. To inhibit water splitting, the EDR system should be operated below the LCD [21]. In this work, LCD was determined using the experimental current-voltage plot. The results of current density vs. voltage is shown in Fig. 2. As illustrated, the operating voltage should be adjusted below 15 V. Therefore, to ensure the operation of EDR stack to be in ohmic region the voltage of 11 V was considered as an upper limit for the subsequent experiments. This voltage is the overall voltage applied to electrodes. Effective voltage is less than these values due to potential drop in electrode chambers [24].

3.2. Results of modeling and optimization by BBD

The matrix of experiments designed by BBD alongside the actual and predicted values of all responses are displayed in Table 6. The results of analysis of variance (ANOVA) for each suggested regression model will be given in flowing sections.

3.2.1. Modeling of desalination efficiency and statistical analysis

A quadratic regression model for the prediction of desalination efficiency vs. voltage (A), flow rate (B) and initial EC (C) has been applied. The reduced form of the suggested model in terms of codded factors is given in Eq. (6).

$$R_1 = +8.52 + 2.65A + 1.28B + 1.33C + 0.79AB + 0.13AC - 1.41BC + 1.39A^2 - 0.69B^2 - 0.6C^2 \quad (6)$$

The results of ANOVA are summarized in Table 7. In general, p-value less than 0.05 demonstrates that a parameter significantly affects the response. Herein, the p-value of the suggested model is less than 0.0001, confirming that the model is highly significant in the studied range of variables. The model F-value of 2,265.12 further indicates the significance level of the model. The terms of all input variables, and mutual interaction terms, including AB, AC and BC, and the second-order effects of parameters, including A^2, B^2 and C^2 are significant with the influence order of $A > C > B > A^2 > BC > AB > B^2 > C^2 > AC$. Moreover, the p-value of lack-of-fit (LoF) is 0.6843, revealing the goodness of fit for the suggested model. The results of other statistical analyses are shown in Table 8. The Adequate Precision of 195.229 is highly greater than 4 and implies that the suggested model can be applied to navigate the design space. The coefficient of variance (C.V.%) is the ratio of standard

Table 4
Quality of brine wastewater from brackish water reverse osmosis process

Characteristics	Value
pH	7.41
Electrical conductivity (μS/cm)	27,300
TDS (ppm)	17,010
Total hardness (ppm)	4,171
Calcium hardness ($CaCO_3$, ppm)	1,612
Mg (ppm)	2,558
Cl (ppm)	7,318
M. ALK ($CaCO_3$, ppm)	189.62
P. ALK ($CaCO_3$, ppm)	0

Table 5
Input variables and their levels for Box–Behnken design modeling

Input variable	Unit	Symbol	Coded and actual levels		
			–1 (low)	0 (medium)	+1 (high)
Applied voltage	V	A	5	8	11
Flow rate	mL/min	B	5	15	25
Electrical conductivity	μS/cm	C	5,000	10,000	15,000

Table 6
Matrix of experiments designed by Box–Behnken design alongside the actual and predicted responses

Run	A	B	C	R_1 (%)		R_2 (mg/m²·s)		R_3 (Wh/L)	
				Actual value	Predicted value	Actual value	Predicted value	Actual value	Predicted value
1	0.00	1.00	–1.00	8.63	8.65	5.51	5.49	0.73	0.72
2	–1.00	–1.00	0.00	6.11	6.15	1.91	1.95	0.03	0.02
3	0.00	–1.00	1.00	8.79	8.76	3.41	3.42	0.79	0.79
4	–1.00	0.00	1.00	7.88	7.86	9.02	8.90	0.35	0.35
5	1.00	–1.00	0.00	9.89	9.87	2.75	2.73	1.23	1.22
6	0.00	0.00	0.00	8.56	8.52	6.63	6.61	0.74	0.74
7	0.00	–1.00	–1.00	3.29	3.28	0.29	0.27	0.21	0.21
8	–1.00	0.00	–1.00	5.5	5.45	2.23	2.22	0.01	0.01
9	1.00	0.00	1.00	13.38	13.42	14.55	14.57	1.72	1.71
10	0.00	0.00	0.00	8.41	8.52	6.5	6.61	0.75	0.74
11	0.00	0.00	0.00	8.54	8.52	6.63	6.61	0.76	0.74
12	1.00	1.00	0.00	14.06	14.01	17.96	17.81	1.66	1.66
13	1.00	0.00	–1.00	10.48	10.49	4.39	4.47	1.34	1.33
14	–1.00	1.00	0.00	7.12	7.13	9.05	9.08	0.18	0.18
15	0.00	1.00	1.00	8.51	8.51	17.65	17.76	0.88	0.87
16	0.00	0.00	0.00	8.62	8.52	6.75	6.61	0.75	0.74
17	0.00	0.00	0.00	8.48	8.52	6.54	6.61	0.74	0.74

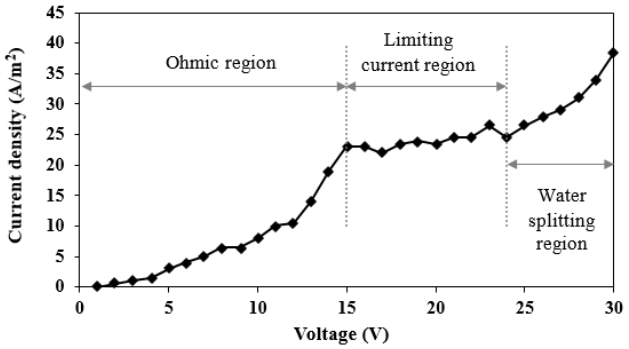

Fig. 2. Results of current density vs. voltage for determination of limiting current density.

deviation to the mean. The lower the coefficient of variance, the higher the accuracy of experiments. The C.V.% of 0.83 verifies the precision of experimental results. Coefficient of determination (R^2) is another tool for evaluating the fitting quality of a regression model. The Pred-R^2 of 0.9980 is in reasonable agreement with the Adj-R^2 of 0.9992, and both of them are so close to 1. Thus, the model is reliable enough for the prediction of desalination efficiency in the studied range of variables. Normal probability and predicted vs. actual are two diagnostic plots for evaluation of regression models. It is evident from Fig. 3a that the residuals follow a normal distribution. Besides, the predicted vs. actual plot given in Fig. 3b depicts that the model predicts the experimental values with high accuracy. In additon, data points are well scattered around the reference line, confirming the assumption of constant variance.

To evaluate the effect of each input variable on the desalination efficiency, the one-factor effect plots are shown in Fig. 4a–c. The other input variables are considered at their medium levels to prevent the extreme effects of them on the response. The desalination efficiency is a strong function of the applied voltage. By increasing applied voltage from 5 up to 11 V, the desalination efficiency is persistently accelerated. The higher applied voltage, the greater driving force for ions to move and pass through the ion exchange membranes [25]. In terms of flow rate and initial EC (Fig. 4b and c), it is found that the desalination efficiency increases slightly when they increase and then tends to be steady at the high levels of input variables. By increasing flow rate, the frequency of solution exposure to the electrical filed increases due to faster liquid circulation, which results in increased ions availability for migration and exchange. Moreover, increasing flow rate leads to the rise in Reynolds number, which increases the desalination efficiency because of suppression of concentration polarization effect [26,27]. However, when flow rate is adjusted at the high level of 25 mL/min, the residence time of the ions significantly reduces and accordingly the ion migration rate is diminished. A similar trend is observed for the effect of initial EC on the desalination efficiency. The desalination efficiency increases when initial EC increases and then it reaches plateau because of increasing mass transfer resistance.

The 3-dimensional (3D) surface plots of desalination efficiency as a function of two independent variables are shown in Fig. 5. From Fig. 5a, the best desalination efficiency in a continues process can be obtained where both the applied voltage and flow rate are in the high levels. While both voltage and flow rate have an effect on desalination efficiency in electrodialysis reversal systems, voltage

Table 7
Results of analysis of variance for desalination efficiency modeling

Source	Sum of squares	df	Mean square	*F*-value	*p*-value Prob. > *F*
Model	104.64	9	11.63	2,265.12	<0.0001
A-Voltage	56.18	1	56.18	10,945.17	<0.0001
B-Flow rate	13.11	1	13.11	2,553.59	<0.0001
C-Electrical conductivity	14.20	1	14.20	2,767.36	<0.0001
AB	2.50	1	2.50	486.36	<0.0001
AC	0.068	1	0.068	13.17	0.0084
BC	7.90	1	7.90	1,538.34	<0.0001
A^2	8.12	1	8.12	1,582.64	<0.0001
B^2	1.60	1	1.60	311.27	<0.0001
C^2	1.52	1	1.52	296.30	<0.0001
Residual	0.036	7	5.133E-003		
Lack of fit	0.010	3	3.417E-003	0.53	0.6843
Pure error	0.026	4	6.420E-003		
Cor. total	104.67	16			

Table 8
Results of other statistical analyses for desalination efficiency modeling

Statistical analysis	Value
Std. Dev	0.072
Mean	8.60
C.V.%	0.83
PRESS	0.20
Adeq. precision	195.229
R^2	0.9997
Adj-R^2	0.9992
Pred-R^2	0.9980

increases have a greater impact on desalination efficiency than flow rate increases [28,29]. This is because increasing the voltage increases the electric current and the potential difference between the electrodes, causing faster movement of ions toward the electrodes [29]. This movement reduces the ion concentration in the dilute channels and consequently reduces the electrolyte conductivity of the solution [28]. Therefore, desalination efficiency increases with increasing voltage up to a subcritical value [29]. Therefore, it may depend on the specific operating conditions and process parameters of the electrodialysis reversal system, but in general, voltage seems to have a higher effect on desalination efficiency than flow rate.

The adequate driving force for overcoming the mass transfer resistance and interruption of concentration polarization leads to the increasing desalination efficiency. Fig. 5b demonstrates that the desalination efficiency reaches the maximum value when both applied voltage and initial EC are at high levels. When initial EC is at the high level, it can be said that there is a concentration gradient promoting mass transfer. The curvature of desalination efficiency plot vs. flow rate and initial EC (Fig. 5c) demonstrates that the best value of desalination efficiency can be obtained when both input variables are adjusted at somewhere between the medium and high levels.

3.2.2. Modeling of ion mass flux and statistical validation

As can be seen from Table 6, the results of ion mass flux are in the range of 0.29 to 17.96, and the maximum to minimum ratio is 61.931. A ratio greater than 10 indicates a transformation is required. Herein, square root transform is suitable to achieve a significant modeling. BBD suggests a quadratic model for prediction of square root of ion mass flux as a function of applied voltage (*A*), flow rate (*B*) and initial feed electrical conductivity (*C*). The reduced form of the suggested model in terms of codded factors is given in Eq. (7).

$$\mathrm{Sqrt}\left(R_2\right) = +2.57 + 0.36A + 1.05B + 0.8C + 0.24AB + 0.052AC + 0.14BC + 0.18A^2 - 0.18B^2 - 0.15C^2 \quad (7)$$

The results of ANOVA for the modeling of square root of ion mass flux are shown in Table 9. Based on the *p*-value and *F*-values, the suggested model is highly significant. Moreover, all first-order input variables alongside the mutual interactions of *AB*, *AC* and *BC*, and the second-order effects of A^2, B^2 and C^2 are significant with the significance order of $B > C > A > AB > A^2 \approx B^2 > C^2 > BC > AC$. The non-significant level of LoF with a *p*-value of 0.2924 reveals that the model can fit the experimental data well. The results of other statistical analyses for the modeling of desalination efficiency are given in Table 10. The adequate precision of 222.601 confirms an adequate signal to navigate the design space. The C.V.% of 0.87 implies the accuracy of the regression model. The Adj-R^2 of 0.9995 and Pred-R^2 of 0.9979 further confirm the capability of the model to predict the square root of ion mass flux in the studied range. The normal probability and predicted vs. actual plots are displayed in Fig. 3c and d. The normal probability plot exhibits that the residuals follow a normal distribution. Also, the

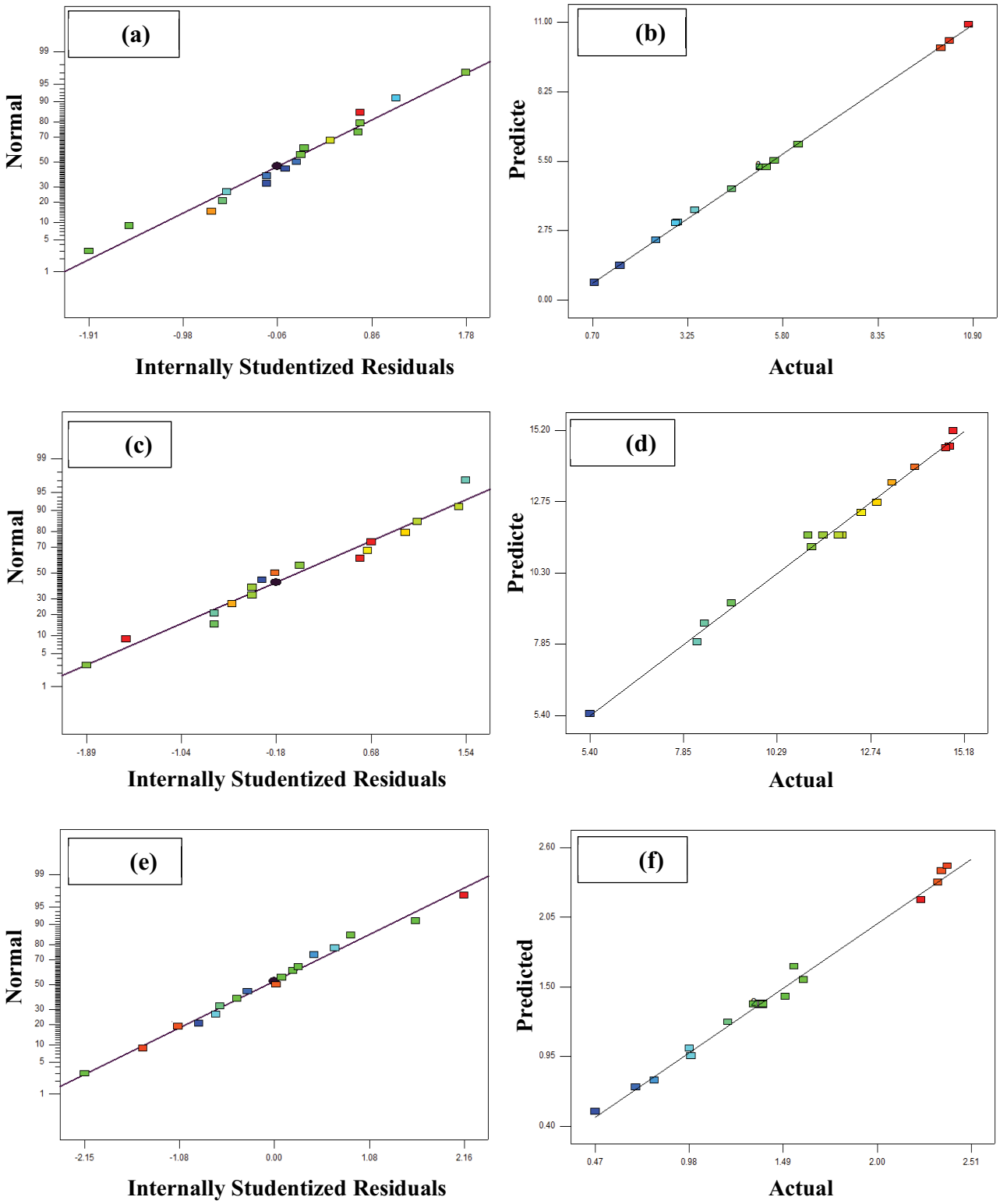

Fig. 3. (a,c,e) Normal probability and (b,d,f) predicted vs. actual plots for the regression models of desalination efficiency, ion mass flux and energy consumption, respectively.

predicted vs. actual plot demonstrates that the predicted responses from the regression model are consistent with the responses from the experimental observations.

To assess the effects of input variables on the ion mass flux, the plots of one-factor effects are shown in Fig. 4d–f. The other variables are kept constant at the medium levels. It

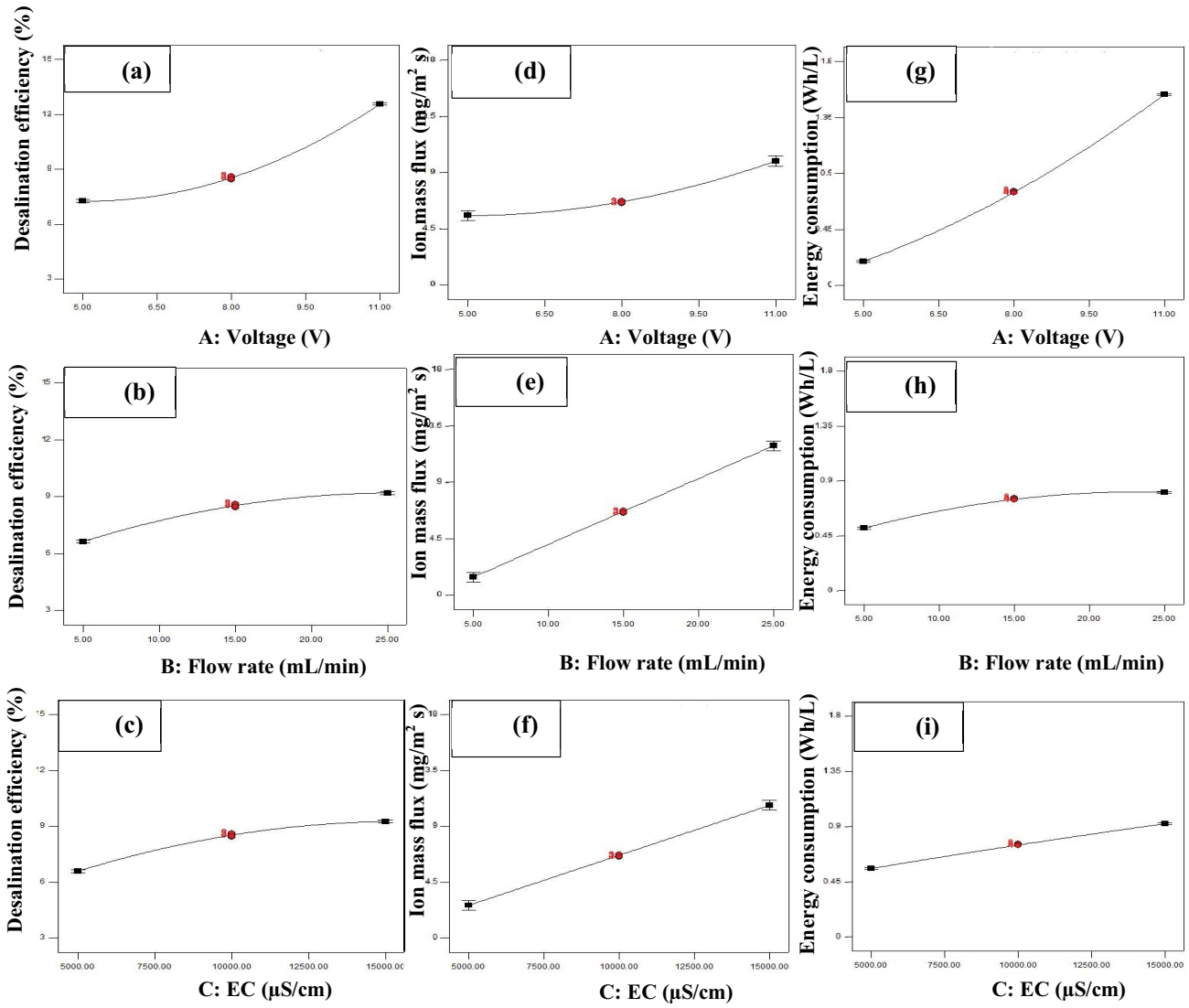

Fig. 4. One-factor plots of (a,d,g) applied voltage, (b,e,h) flow rate, and (c,f,i) electrical conductivity on the desalination efficiency, ion mass flux and energy consumption, respectively.

is apparent from Fig. 4d that increasing the applied voltage from 0 up to 11 V increases the ion mass flux, because the applied voltage is indeed the driving force of ion migration [21]. Based on the Nerst–Plunck equation [30], the electromigration of the ions is propotional to gradient of applied voltage, thus it is reasonable that ion mass flux enhances with the increment of applied voltage. Flow rate and initial EC also affect the ion mass flux, as shown in Fig. 4e and f. The increment of flow rate results in the increasing the ion mass flux. Flow rate can affect mass transfer coefficient so that a higher flow rate leads to the enhancement of mass transfer flux. A similar trend is observed for the variation of initial EC. The best value of ion mass flux is obtained at maximum value of initial EC.

The results of ANOVA confirmed the mutual interaction of *AB*, *AC* and *BC*. Fig. 6 depicts the 3D surface plots of square root of ion mass flux influenced by the simultaneous variation of independent variables. The other input variable is kept constant at the medium level. As can be seen from Fig. 6a, the best ion mass flux can be obtained by adjusting both applied voltage and flow rate at high levels. The high value of voltage can support the driving force of ion migration even when the residence time of ions is at the minimum level.

Despite some slight differences, the 3D plots of square root of ion mass flux and desalination efficiency have a similar curvature, and the best results of ion mass flux and desalination efficiency are obtained at the same values of input variables. It is reasonable that the higher desalination efficiency is a result of higher ion mass flux. Fig. 6b indicates that the ion mass flux can be maximized by adjusting both applied voltage and initial EC at the high levels. Fig. 6c illustrates the 3D plot of square root of ion mass flux as a function of flow rate and initial EC. The best response is obtained when both flow rate and initial EC are at the high levels. These results are in agreement

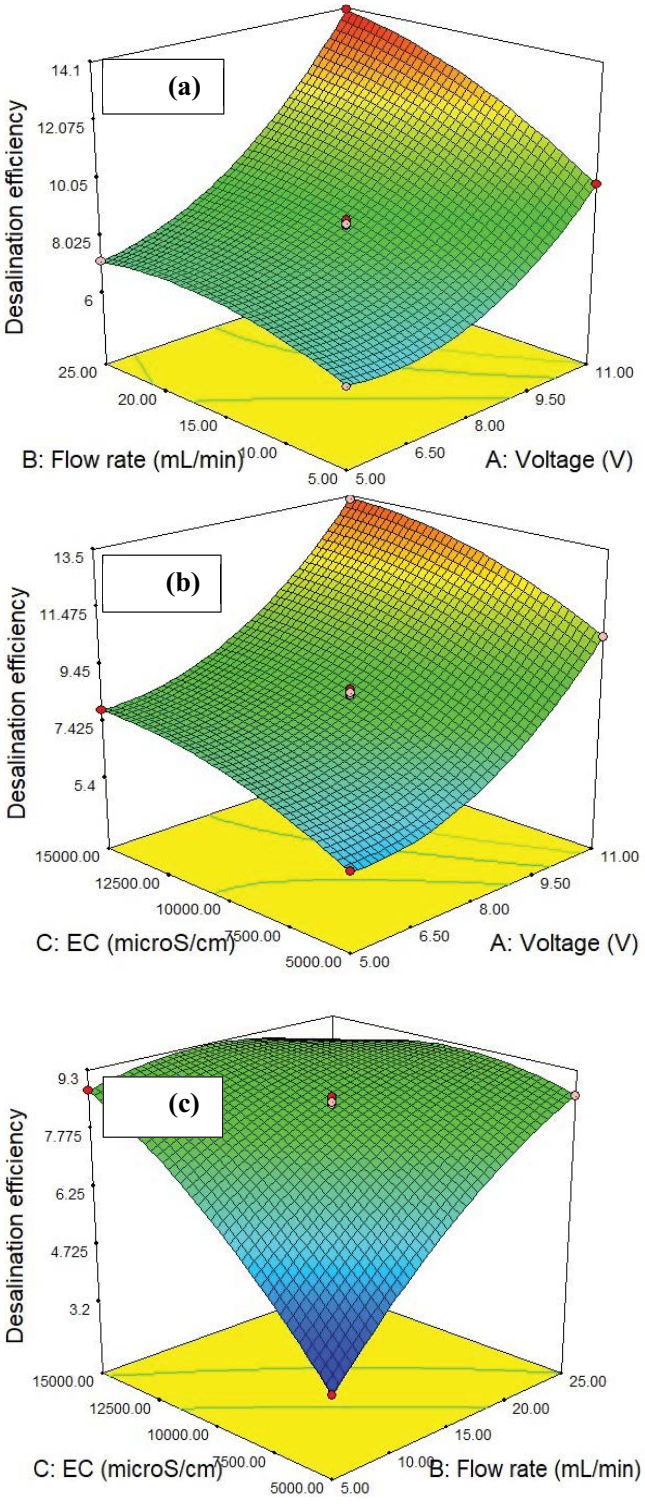

Fig. 5. 3-Dimensional plot of desalination efficiency as a function of independent variables of (a) applied voltage-flow rate, (b) applied voltage-initial electrical conductivity, and (c) flow rate-initial electrical conductivity.

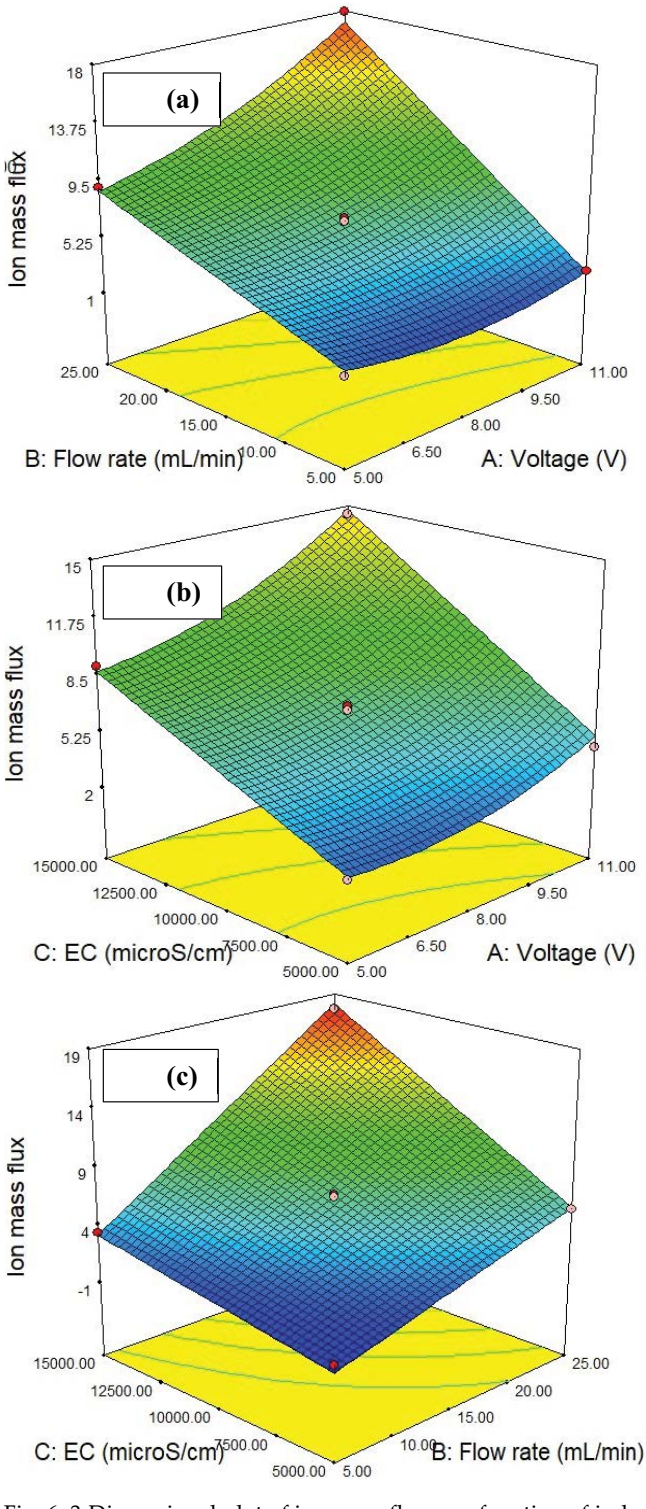

Fig. 6. 3-Dimensional plot of ion mass flux as a function of independent variables of (a) applied voltage-flow rate, (b) applied voltage-initial electrical conductivity, and (c) flow rate-initial electrical conductivity.

with the results obtained from the regression modeling of desalination efficiency. While both voltage and flow rate have an effect on ion mass flux and desalination efficiency in electrodialysis reversal systems, flow rate increases have a greater impact on mass flux and mass transfer coefficient than voltage increases [28,31]. This is because increasing the current density by increasing the voltage

Table 9
Results of analysis of variance for square root of ion mass flux modeling

Source	Sum of squares	df	Mean square	*F*-value	*p*-value Prob. > *F*
Model	15.61	9	1.73	3,700.52	<0.0001
A-Voltage	1.07	1	1.07	2,272.20	<0.0001
B-Flow rate	8.76	1	8.76	18,680.17	<0.0001
C-Electrical conductivity	5.11	1	5.11	10,893.43	<0.0001
AB	0.23	1	0.23	484.74	<0.0001
AC	0.011	1	0.011	23.34	0.0019
BC	0.074	1	0.074	158.86	<0.0001
A^2	0.14	1	0.14	305.58	<0.0001
B^2	0.14	1	0.14	303.24	<0.0001
C^2	0.100	1	0.100	212.47	<0.0001
Residual	3.281E-003	7	4.687E-004		
Lack of fit	1.869E-003	3	6.231E-004	1.77	0.2924
Pure error	1.412E-003	4	3.529E-004		
Cor. total	15.61	16			

Table 10
Results of other statistical analyses for square root of ion mass flux modeling

Statistical analysis	Value
Std. Dev	0.022
Mean	2.50
C.V.%	0.87
PRESS	0.032
Adeq. precision	222.601
R^2	0.9998
Adj-R^2	0.9995
Pred-R^2	0.9979

may cause limitations due to concentration polarization [a]. On the other hand, increasing the flow rate may enhance the mass transport by reducing the boundary layer thickness and increasing the turbulence [32]. Therefore, it may depend on the specific operating conditions and process parameters of the electrodialysis reversal system, but in general, flow rate seems to have a higher effect on ion mass flux and desalination efficiency than voltage.

3.2.3. Modeling of energy consumption and statistical validation

The third response of this process is energy consumption which is vital to be minimize for realization of the

Table 11
Results of analysis of variance for energy consumption modeling

Source	Sum of squares	df	Mean square	*F*-value	*p*-value Prob. > *F*
Model	4.21	9	0.47	7,192.99	<0.0001
A-Voltage	3.62	1	3.62	55,662.31	<0.0001
B-Flow rate	0.18	1	0.18	2,723.27	<0.0001
C-Electrical conductivity	0.26	1	0.26	4,043.27	<0.0001
AB	0.020	1	0.020	301.54	<0.0001
AC	4.000E-004	1	4.000E-004	6.15	0.0422
BC	0.046	1	0.046	711.15	<0.0001
A^2	0.055	1	0.055	852.96	<0.0001
B^2	0.032	1	0.032	498.79	<0.0001
C^2	2.529E-004	1	2.529E-004	3.89	0.0892
Residual	4.550E-004	7	6.500E-005		
Lack of fit	1.750E-004	3	5.833E-005	0.83	0.5413
Pure error	2.800E-004	4	7.000E-005		
Cor. total	4.21	16			

Table 12
Results of other statistical analyses for energy consumption modeling

Statistical analysis	Value
Std. Dev	0.008
Mean	0.76
C.V.%	1.06
PRESS	0.003
Adeq. precision	276.139
R^2	0.9999
Adj-R^2	0.9998
Pred-R^2	0.9992

process. The energy consumption model sugeested by BBD is quadratic, and its codded form is given in Eq. (8).

$$R_3 = +0.75 + 0.67A + 0.15B + 0.018C + 0.07AB + 0.01AC - 0.11BC + 0.11A^2 + -0.088B^2 - 0.0077C^2 \quad (8)$$

The results of ANOVA (Table 11) demonstrate the highly significance level of the model with p-value lower than 0.0001 and F-value of 7,192.99 [29,30]. With p-value lower than 0.05, the input variables of A, B and C, the mutual interactions of AC, AC and BC, and the second-order effect of A^2, B^2 and C^2 are significant terms for the modeling of energy consumption. Based on the F-values, the significance order of $A > C > B > A^2 > BC > B^2 > AB > AC > C^2$ is deduced. The p-value of 0.5413 exhibits that the LoF is non-significant and thereby the model is capable to fit the experimental data. Moreover, from Table 12, the adequate precision of 276.139 and C.V.% of 1.06 are high and low enough, respectively. The Pred-R^2 of 0.9992 is in reasonable agreement with the Adj-R^2 of 0.9998. The normal probability and predicted vs. actual plots are displayed in Fig. 3e and f to diagnosis the validity of the regression model of energy consumption. Fig. 3e displays that the residuals follow a straight line, confirming that the normally distribution of data. As can be seen from Fig. 3f, the predicted and actual points are scattered around the regressed diagonal line, which is in agreement with the high value of Pred-A^2 and indicates that the predictability of the model is satisfactory.

The one-factor plots for energy consumption as a function of each independent variables are given in Fig. 4g–i. It is deduced from Fig. 4g that the applied voltage has a strong effect on the energy consumption. The effects of other input variables, flow rate and initial EC, on the energy consumption are consistent with those on the desalination efficiency because the desalination is a result of ion transfer through the membranes and ion transfer is responsible for generated current. The 3D surface plots showing the effect of mutual interactions of AB, AC and BC on energy consumption are presented in Fig. 7. From Fig. 7a, the energy consumption can be minimized where both applied voltage and flow rate are at low levels. This result verifies the result obtained from the variation of desalination efficiency as a function of applied voltage and flow rate (Fig. 5a). Also, it is seen that the effect of applied voltage is more significant than that

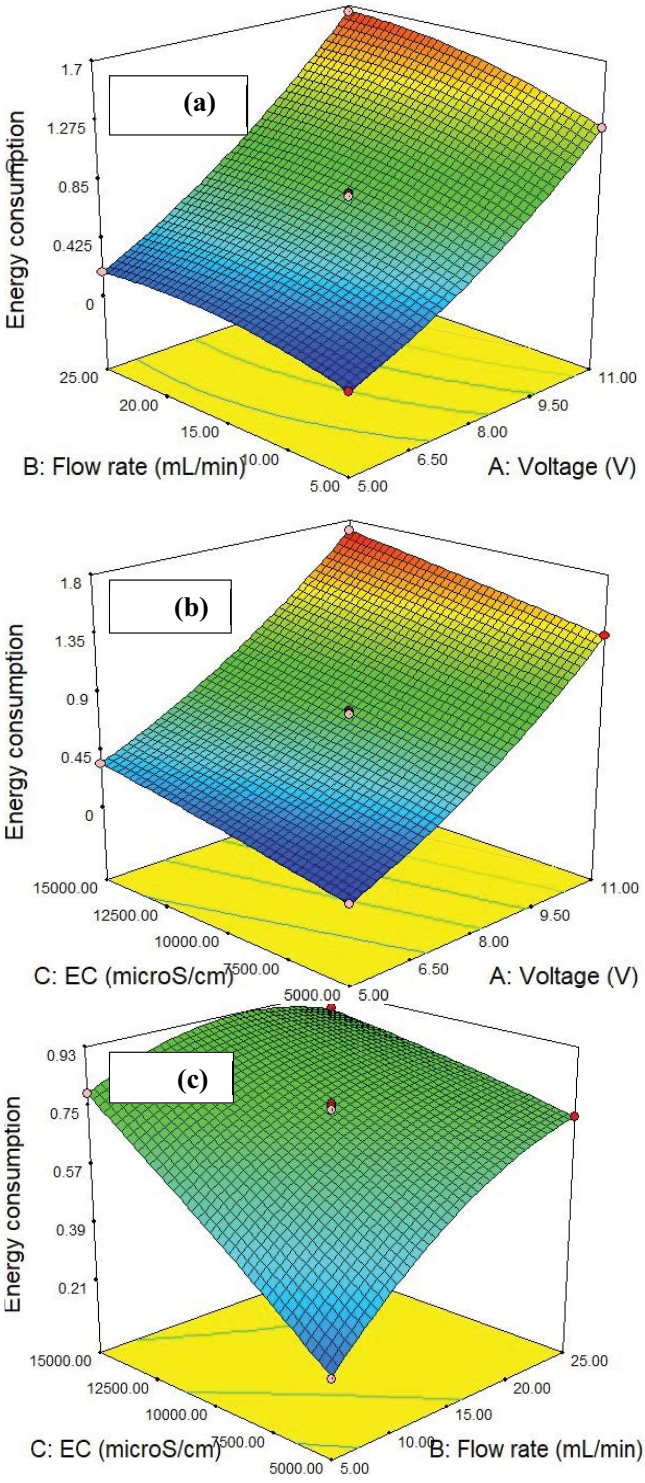

Fig. 7. 3-Dimensional plot of energy consumption as a function of independent variables of (a) applied voltage-flow rate, (b) applied voltage-initial electrical conductivity, and (c) flow rate-initial electrical conductivity.

of flow rate on the energy consumption. Fig. 7b demonstrates that the energy consumption is minimized when both applied voltage and initial EC are at the low levels. Moreover, it is depicted from Fig. 7c that to minimize the

Table 13
Predicted and actual responses at optimum condition

Responses	R_1 (%)	R_2 (mg/m²·s)	R_3 (Wh/L)
Predicted	8.68	15.27	0.80
Actual	8.69	15.25	0.81

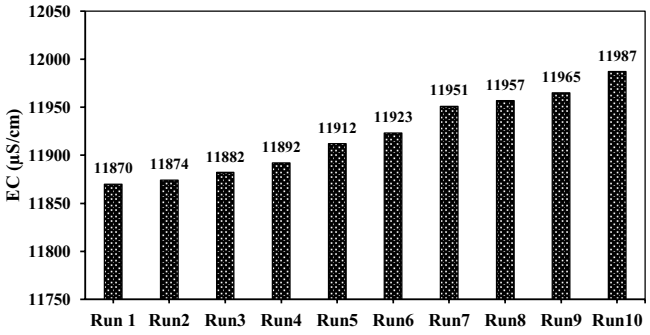

Fig. 8. Results of final electrical conductivity of diluted water after 10 times electrodialysis reversal process at the optimum condition.

energy consumption, both flow rate and initial EC should be adjusted at their lowest levels. Under this circumstance, the current carried by transferred ions is minimized, thus diminishing energy consumption. The results obtained from modeling of energy consumption is in agreement with the results obtained by the modeling of desalination efficiency.

3.2.4. Optimization and verification study

For realization of the waste minimization by EDR process, it is important to find the optimum condition of input variables under which by consuming the lowest amount of energy, the highest desalination efficiency could be achieved. Multi-response optimization was done by adjusting *A*, *B*, and *C* parameters in their defined ranges to maximize both desalination efficiency and ion mass flux, while minimizing energy consumption simultaneously. The optimum condition of applied voltage of 7.7 V, flow rate of 25 mL/min and initial EC of 13,000 µS/cm were found. Table 13 indicates the predicted values of desalination efficiency, ion mass flux, and energy consumption at the optimum condition with desirability of 0.894. An experiment was conducted and triplicated at optimum condition to verify the predicted results. As can be clearly seen from Table 13, the actual values of desalination efficiency, ion mass flux and energy consumption are in reasonable agreement with the predicted values, implying the reliability and accuracy of the models.

3.2.5. Evaluation of self-cleaning effect by reversing polarity

The influence of the polarity reversal time on the process performances was investigated by increasing time from 10 to 60 min. considering all operational parameters 45 min was chosen for the polarity reversal time for all test runs. In order to evaluate the self-cleaning effect of EDR process, under optimum condition, the ED process was performed for 45 min followed by reversing polarity for 15 min, and this process was repeated for 10 times. The final EC of diluted water after each run is shown in Fig. 8. As it can be seen, the EC was diminished from 13,000 up to 11,297 µS/cm for the first run which corresponds to 8.69% desalination efficiency. After 10 times self-cleaning of the membranes via reversing polarity, the desalination efficiency was reduced up to 7.79% which shows that the polarity reversal can significantly help with membrane cleaning.

4. Conclusion

The performance of RO brine minimization using EDR process is highly dependent on the operating parameters. In this study, applied voltage, flow rate and initial EC were studied as independent input variables and desalination efficiency, ion mass flux and energy consumption were considered as the output responses. Box–Behnken experimental design suggested a correlation between the input variables and output responses with high values of Pred-R^2. The desalination efficiency regression model shows the mutual interactions of applied voltage-EC, applied voltage-flow rate and flow rate-EC. It was found that there is a trade-off between the desalination efficiency and energy consumption. The energy consumption regression model was a strong function of applied voltage and the least amount of energy consumption was supported at the lowest value of applied voltage. The optimization conditions for maximizing the desalination efficiency while minimizing energy consumption were obtained to be voltage of 7.7 V, flow rate of 25 mL/min and initial EC of 13,000 µS/cm with the predicted desalination efficiency of 8.68%, ion mass flux of 15.27 mg/m²·s, and energy consumption of 0.8 Wh/L. The actual responses at the optimum conditions verified the reliability and predictability of the models.

References

[1] M. Turek, J. Was, P. Dydo, Brackish water desalination in RO–single pass EDR system, Desal. Water Treat., 7 (2009) 263–266.
[2] S.N. Backer, I. Bouaziz, N. Kallayi, R.T. Thomas, G. Preethikumar, M.S. Takriff, T. Laoui, M.A. Atieh, Brine solution: current status, future management and technology development, Sustainability, 14 (2022) 6752, doi: 10.3390/su14116752.
[3] J. Morillo, J. Usero, D. Rosado, H. El Bakouri, A. Riaza, F.-J. Bernaola, Comparative study of brine management technologies for desalination plants, Desalination, 336 (2014) 32–49.
[4] D. Zhao, L.Y. Lee, S.L. Ong, P. Chowdhury, K.B. Siah, H.Y. Ng, Electrodialysis reversal for industrial reverse osmosis brine treatment, Sep. Purif. Technol., 213 (2019) 339–347.
[5] V.M. Ortiz-Martínez, L. Gómez-Coma, C. Tristán, G. Pérez, M. Fallanza, A. Ortiz, R. Ibáñez, I. Ortiz, A comprehensive study on the effects of operation variables on reverse electrodialysis performance, Desalination, 482 (2020) 114389, doi: 10.1016/j.desal.2020.114389.
[6] M. Vanoppen, E. Criel, G. Walpot, D.A. Vermaas, A. Verliefde, Assisted reverse electrodialysis—principles, mechanisms, and potential, npj Clean Water, 1 (2018) 1–5.
[7] G.D. Enoch, P. Tigchelaar, J. de Niet, J. Lefers, Investigations with electrodialysis reversal for the treatment of surface water to make-up water, Sep. Purif. Technol., 25 (1990) 1387–1406.
[8] L. Karimi, A. Ghassemi, Effects of operating conditions on ion removal from brackish water using a pilot-scale electrodialysis reversal system, Desal. Water Treat., 57 (2016) 8657–8669.

[9] Y. Zhang, K. Ghyselbrecht, R. Vanherpe, B. Meesschaert, L. Pinoy, B. Van der Bruggen, RO concentrate minimization by electrodialysis: techno-economic analysis and environmental concerns, J. Environ. Manage., 107 (2012) 28–36.
[10] K. Kwon, J. Han, B.H. Park, Y. Shin, D. Kim, Brine recovery using reverse electrodialysis in membrane-based desalination processes, Desalination, 362 (2015) 1–10.
[11] M.O. Mavukkandy, C.M. Chabib, I. Mustafa, A. Al Ghaferi, F. AlMarzooqi, Brine management in desalination industry: from waste to resources generation, Desalination, 472 (2019) 114187, doi: 10.1016/j.desal.2019.114187.
[12] K. Ghyselbrecht, E. Van Houtte, L. Pinoy, J. Verbauwhede, B. Van der Bruggen, B. Meesschaert, Treatment of RO concentrate by means of a combination of a willow field and electrodialysis, Resour. Conserv. Recycl., 65 (2012) 116–123.
[13] D. Ariono, M. Purwasasmita, I.G. Wenten, Brine effluents: characteristics, environmental impacts, and their handling, J. Eng. Sci. Technol., 48 (2016) 367–387.
[14] C. Jiang, Y. Wang, Z. Zhang, T. Xu, Electrodialysis of concentrated brine from RO plant to produce coarse salt and freshwater, J. Membr. Sci., 450 (2014) 323–330.
[15] J. Steger, South Bay Water Reclamation Plant and Ocean Outfall Pretreatment Annual Report, Environmental Monitoring and Technical Services, Public Utilities Department, City of San Diego, USA, 2020. Available at: https://www.sandiego.gov/sites/default/files/19_sb_annual_report.pdf
[16] M. Steirer, A. Dorman, A. Van, J. Pasek, W. Pearce, A. Rife, J. Quicho, L. Chou, Indirect Potable Reuse/Reservoir Augmentation Demonstration Project, Advanced Water Purification Facility (AWPF) Study Report, City of San Diego, USA, 2013. Available at: https://www.sandiego.gov/sites/default/files/legacy/water/purewater/pdf/projectreports/awpfstudyreport.pdf
[17] H. Kim, S. Yang, J. Choi, J.-O. Kim, N. Jeong, Optimization of the number of cell pairs to design efficient reverse electrodialysis stack, Desalination, 497 (2021) 114676, doi: 10.1016/j.desal.2020.114676.
[18] S. Caprarescu, V. Purcar, D.-I. Vaireanu, Separation of copper ions from synthetically prepared electroplating wastewater at different operating conditions using electrodialysis, Sep. Sci. Technol., 47 (2012) 2273–2280.
[19] N. Kabay, M. Yüksel, S. Samatya, Ö. Arar, Ü. Yüksel, Effect of process parameters on separation performance of nitrate by electrodialysis, Sep. Sci. Technol., 41 (2006) 3201–3211.
[20] R. Valerdi-Pérez, L.M. Berná-Amorós, J.A. Ibáñez-Mengual, Determination of the working optimum parameters for an electrodialysis reversal pilot plant, Sep. Sci. Technol., 35 (2000) 651–666.
[21] L. Karimi, A. Ghassemi, An empirical/theoretical model with dimensionless numbers to predict the performance of electrodialysis systems on the basis of operating conditions, Water Res., 98 (2016) 270–279.
[22] Y. Xu, Y. Sun, Z. Ma, R. Wang, X. Wang, J. Wang, L. Wang, X. Gao, J. Gao, Response surface modeling and optimization of electrodialysis for reclamation of RO concentrates in coal-fired power plants, Sep. Sci. Technol., 55 (2020) 2593–2603.
[23] M. Wang, K.-k. Wang, Y.-x. Jia, Q.-c. Ren, The reclamation of brine generated from desalination process by bipolar membrane electrodialysis, J. Membr. Sci., 452 (2014) 54–61.
[24] S. Thirumalini, K. Joseph, Correlation between electrical conductivity and total dissolved solids in natural waters, Malaysian J. Sci., 28 (2009) 55–61.
[25] N. Káňavová, L. Machuča, D. Tvrzník, Determination of limiting current density for different electrodialysis modules, Chem. Pap., 68 (2014) 324–329.
[26] P. Długołęcki, P. Ogonowski, S.J. Metz, M. Saakes, K. Nijmeijer, M. Wessling, On the resistances of membrane, diffusion boundary layer and double layer in ion exchange membrane transport, J. Membr. Sci., 349 (2010) 369–379.
[27] J. Liu, J. Yuan, Z. Ji, B. Wang, Y. Hao, X. Guo, Concentrating brine from seawater desalination process by nanofiltration–electrodialysis integrated membrane technology, Desalination, 390 (2016) 53–61.
[28] S.K. Patel, M. Qin, W.S. Walker, M. Elimelech, Energy efficiency of electro-driven brackish water desalination: electrodialysis significantly outperforms membrane capacitive deionization, Environ. Sci. Technol., 54 (2020) 3663–3677.
[28] W. Lee, A-C.L. Henaff, S. Amrose, T. Buonassisi, I.M. Peters, Voltage- and flow-controlled electrodialysis batch operation: flexible and optimized brackish water desalination, Desalination, 500 (2021) 114837, doi: 10.1016/j.desal.2020.114837.
[30] B. Chen, C. Jiang, Y. Wang, R. Fu, Z. Liu, T. Xu, Selectrodialysis with bipolar membrane for the reclamation of concentrated brine from RO plant, Desalination, 442 (2018) 8–15.
[31] M. Sadeghi, M. Mahdi Behvand Usefi, A.F. Ismail, M. Ghasemi, Environmental sustainability and ions removal through electrodialysis desalination: operating conditions and process parameters, Desalination, 549 (2023) 116319, doi: 10.1016/j.desal.2022.116319.
[32] L.M. Camacho, J.A. Fox, J.O. Ajedegba, Optimization of electrodialysis metathesis (EDM) desalination using factorial design methodology, Desalination, 403 (2017) 136–143.